Large and Complex Velocity Models Using 3D Tomographic MVA

Paul Docherty, Mike Plumlee, Mike Sullivan, Robert Windels, Scott Tiefenthaller and John Anderson*, Fairfield Industries, Inc.

Summary

The development of velocity models over large and complex areas can be the prohibitive cost and time portion of depth imaging due to limited resources for interpreting velocity errors. Fairfield Industries Inc. have developed a tomographic procedure that addresses these issues. This procedure incorporates a flexible model parameterization, sparse ray tracing for traveltime approximations, automatic detection of residual moveout, parallel algorithm design, and image computation in the direction normal to reflectors.

Introduction

Fairfield Industries Inc. Tomographic techniques aim to bring about the horizontal alignment by adjusting velocity along rays traced through the model. Difficulties in 3-D arise from the size of the problem: poorly parameterized models can become too large to fit in memory, and the data volume involved is typically enormous, resulting in prohibitive run times. Additionally, manual estimation of curvature in the gathers can become cumbersome in 3-D or the manual estimates become too sparse to define the velocity field adequately. Building on the innovative work of many authors, we address these issues and illustrate our technique with a large dataset example from the Gulf of Mexico.

Model Parameterization

The model consists of regions, typically of smoothly varying velocity, and their boundaries in either time or depth. Following Farmer et al. (1994), each region is parameterized independently; for example, a model might contain a tessellated overburden region, a salt body described by a constant, and a subsalt region with depth-dependent variation. In good data areas, region boundaries are picked in the time domain and converted to depth using ray methods; otherwise, they are obtained from preliminary depth images. Instructions accompany the boundaries to indicate how the regions fit together to make the model: in essence, given $\mathbf{x} = (x,y,z)$ they identify the region i containing $\mathbf{x}$, enabling the velocity $v(\mathbf{x}) = v_i(\mathbf{x})$ to be extracted.

Velocity Analysis Procedure

Like other MVA methods, our procedure follows three basic steps: (i) at locations distributed throughout the model compute depth migrated image gathers; (ii) estimate the traveltime corrections necessary to flatten the gathers; (iii) solve a large system of equations to simultaneously obtain velocity updates throughout the model (so-called global tomography).

Image Gather Locations

As in Wyatt et al. (1997) we prefer to concentrate our image gather calculations in the neighborhood of reflectors. Target reflectors are typically chosen on a time migration, mapped to depth using the current velocity, and then divided into a regular mesh of points. The mesh points are locations where image gathers are to be computed; however, unlike the conventional practice of computing gathers in a vertical window, we choose to align the image window in the direction of the normal to the reflector at each gather location. In doing so we avoid a loss of frequency in the image that is proportional to the cosine of reflector dip (Schneider, 1978). Stated differently (Bleistein 1987), the output $\gamma(\mathbf{x})$ of a depth migration in the neighborhood of a reflector is a band-limited delta function with support on the reflector: $\gamma(\mathbf{x}) = R\ \delta(s)$, where s measures arc length *normal to the reflector* and R is the angularly dependent reflection coefficient. Not only do we obtain the highest frequency migrated image in the direction normal to the reflector, but also at the lowest cost, since we can use a shorter image window.

Traveltime corrections

For each image gather we trace rays from only a single point (at the center of the image window) and use paraxial approximations to obtain the additional traveltimes required. (Typically our image window is several hundred meters in extent.) Instead of attempting to measure the curvature, or depth errors, in the gather, we employ the scanning technique described in Audebert et al. (1996). There the authors pointed out that multiplication of the entire velocity field by a constant, α, causes the traveltimes to change by a factor $1/\alpha$, since the raypaths are unaffected. Recomputing the image gather for a range of values of α is thus particularly straightforward, at least in terms of the traveltimes. Scanning within a specified range, for example $0.90 \le \alpha \le 1.10$, we compute the horizontal semblance, or flatness, of the image gather for each value of α. From the value of α that gives the maximum semblance we obtain the traveltime correction to be used in the inversion: $\delta T = T - T/\alpha$ where T is the traveltime along a ray associated with this image gather location. Audebert et al. in their 1997 paper suggested that these traveltime corrections might be used for a full 3-D tomographic inversion.

Tomographic update

Each image gather contributes rays to the tomographic matrix. We use a standard row action method (Stewart, 1991) to solve the system of equations. Additionally, the equations corresponding to each gather are assigned a weight equal to the maximum semblance realized in the

velocity scan, in effect reducing the influence of poor quality gathers on the inversion result. One or more regions that are to be updated are specified and corrections appropriate to their parameterizations are computed.

Implementation

In order to be feasible on 3-D data sets the algorithm is implemented in parallel. In our design all of the processors receive a copy of the velocity model. Likewise, all of the processors receive the same seismic data: all, or a significant part of, the 3-D survey. Parallelization occurs in the output space where the image gather locations are divided among the processors. In an initialization phase, each processor computes raypaths for its set of gathers (recall that rays are traced from only a single point for each gather). Next, on receiving an ensemble of data, a processor immediately depth migrates it into its portion of the output space: not only at the current velocity, but also at all of the scaled velocities making up the velocity scan. Once all of the data has been accessed, the gather semblances are computed and for each gather the value of α providing the maximum semblance is retrieved. Finally, the tomographic matrix is inverted and the whole procedure is iterated, usually several times.

Example

Our 3D examples are of a salt intrusion, and a tertiary section from the Gulf of Mexico shelf off Louisiana. Survey areas are approximately 210 square kilometers and 5200 square kilometers, respectively. The starting point for the analysis was an interpreted prestack time migration, along with velocities from conventional time processing. The starting depth model contained a gridded overburden obtained by depth converting the time velocities; and for the salt example a constant velocity region flooded to the base of the model at 30,000 ft. The top of salt, which divides the two velocity regions, was obtained from image ray calculations. Starting salt velocity was taken to be 14,000 fts^{-1}.

Image gather locations were specified several horizons and on portions of the base-salt reflection, which could also be interpreted in some parts of the time migration. In each case tens of thousands of image gather locations were identified. (Each horizon was divided into a mesh of gather locations.) Figure 1 shows the gather locations for the top of salt, the normals indicating the direction of the image calculation.

In the first iteration of the tomographic inversion the goal is to refine the velocities tertiary section and when salt is present simultaneously obtaining a better estimate of the velocity within the salt. There were multiple updates in the overburden velocity and the velocity near the salt boundary where the salt velocity had bled into neighboring sediments in the input model. After a few iterations of tomography, the specified horizons were reinterpreted in depth before proceeding with the next series of tomography. This procedure is repeated until the velocities converge to an acceptable level.

When salt was present, the base of salt was sought using prestack depth migration of a fairly coarse grid of lines. (The velocity model, though updated by tomography, still contains a salt flood at this stage.) Figure 2 shows one of the migrated output lines. The base-salt reflection suggests that the salt may be disconnected from its stock at depth. Picking the salt boundary and incorporating it into the model leaves only the subsalt velocities to be determined. Rather than introduce a new, independently parameterized, subsalt region where previously the salt flood had existed, we choose to continue with a two-region model, extending our overburden grid into the subsalt zone. (Grid velocities below the salt are initialized with grid values at the same depth, but away from the salt.) Since little can be interpreted beneath the salt, it is difficult, or impossible, to target our image gather computations in this zone. Instead, we simply lay down a regular mesh of gather locations, repeated at depths of interest, and point the corresponding normals in the direction of the upward pointing vertical.

In the next iterations of tomography, the matrix is thus derived from image gathers located in the overburden section and we continue to seek refinements for the salt velocity as well. Interestingly, the latter iterations can be made relatively inexpensive. For example, if gathers in the overburden have appeared flat in previous iterations, and if the corresponding rows in the matrix have been saved, then it seems reasonable that these values can be used again; that is, it may not be necessary to repeat many of the image gather computations. The reason is that raypaths and traveltimes are unlikely to change substantially in parts of the model where velocities are close to converging on their true values. Figures 3 and

Conclusions

Taking advantage of a flexible model parameterization and using only sparse ray calculations, we are able to obtain both accurate and efficient tomographic velocity inversions. The troublesome procedure of estimating residual curvature on image gathers, which in 2-D has traditionally been carried out manually, is accomplished automatically with this tomographic approach. The method is aptly suited to parallel implementation and is designed for application to very large data sets.

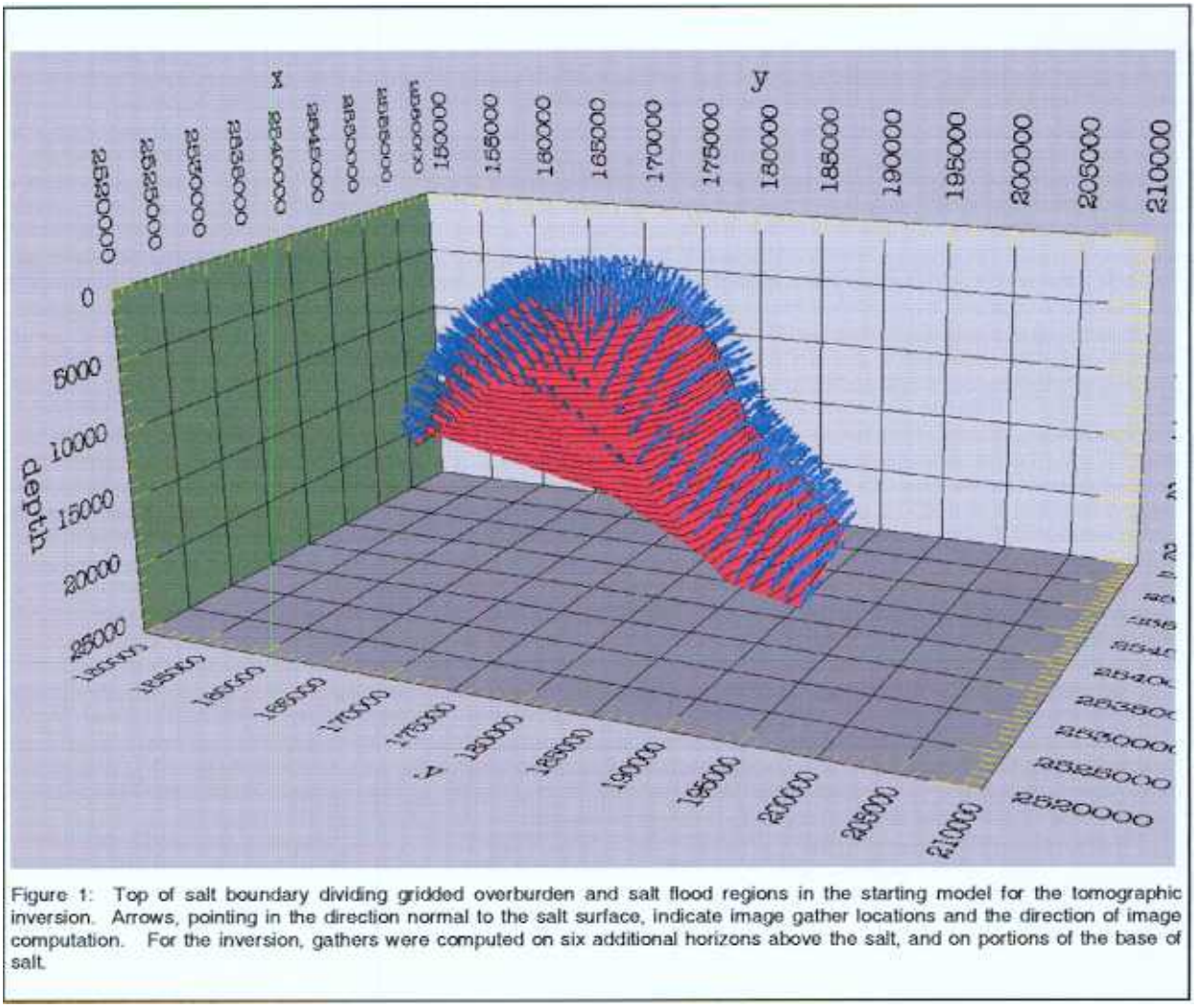

Figure 1: Top of salt boundary dividing gridded overburden and salt flood regions in the starting model for the tomographic inversion. Arrows, pointing in the direction normal to the salt surface, indicate image gather locations and the direction of image computation. For the inversion, gathers were computed on six additional horizons above the salt, and on portions of the base of salt.

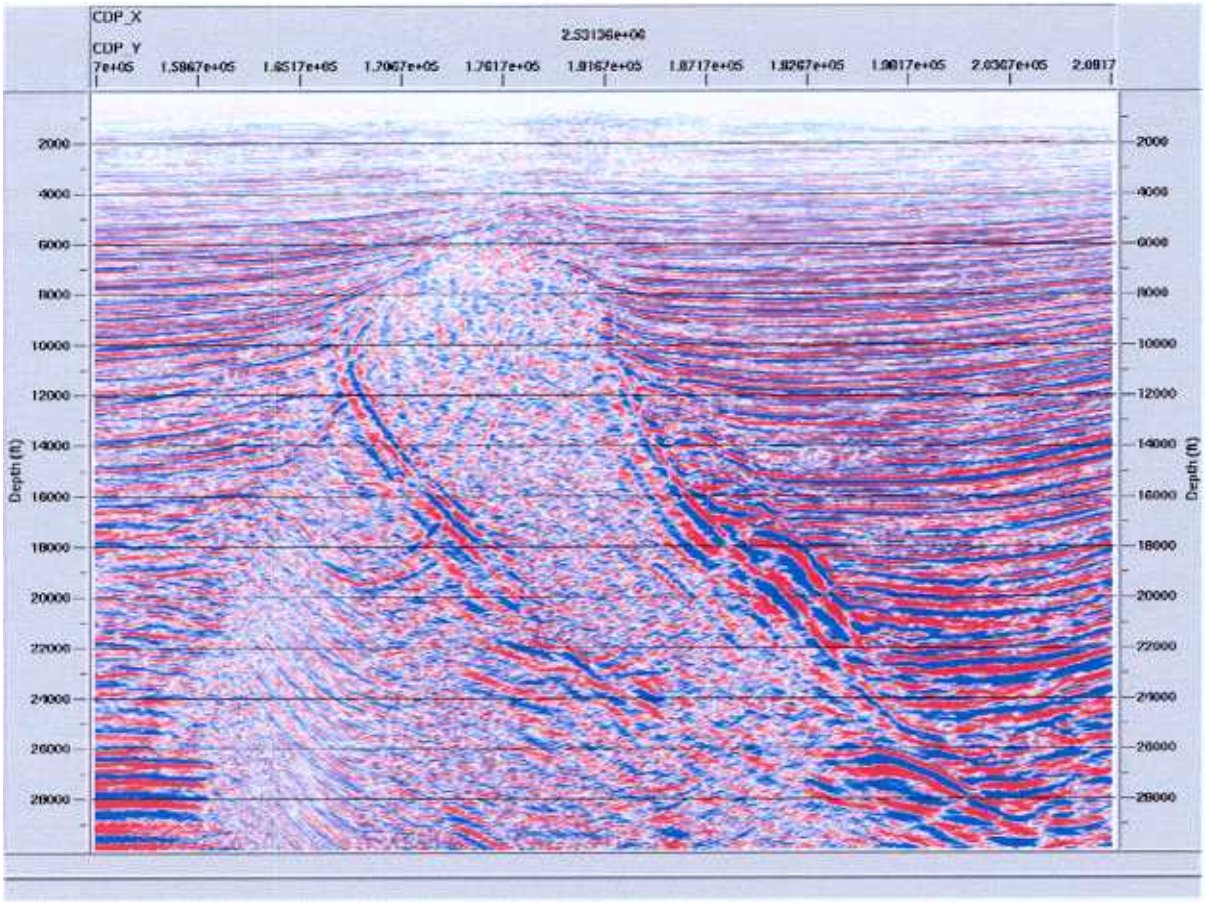

Figure 2: 3-D prestack depth migration of one of the target lines used to interpret the base of salt. The velocity model, which still contains a salt flood at this stage, was obtained from the first iteration of tomography. In relation to Figure 1, the line is at constant x and has a length of 55,000 ft.

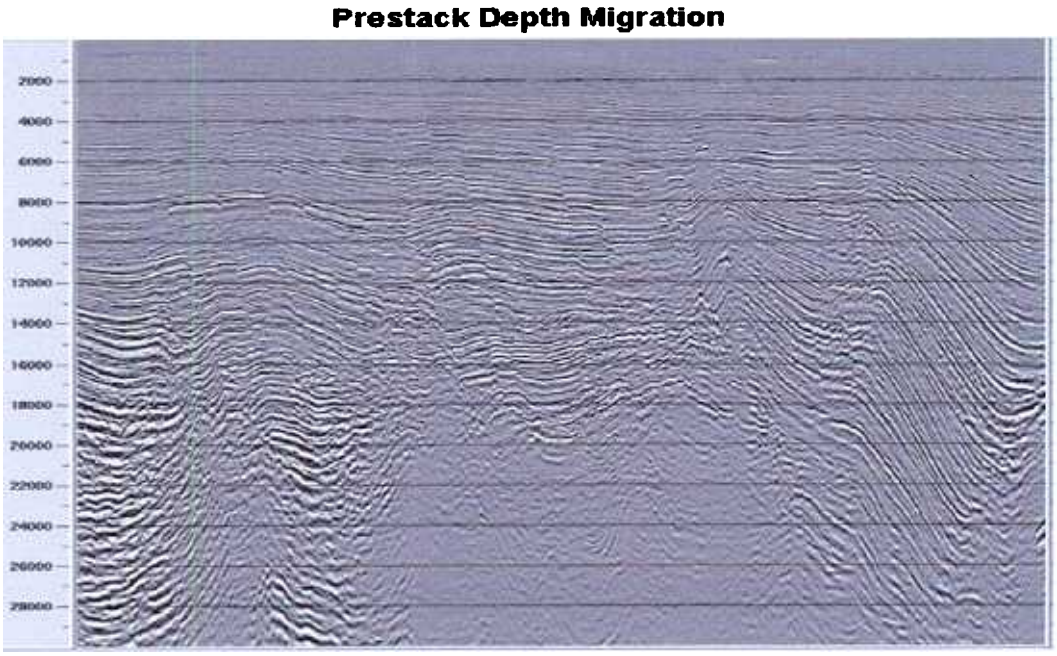

Figure 3 : Preliminary output of 3D Kirchhoff prestack depth migration Target In-Line 4200

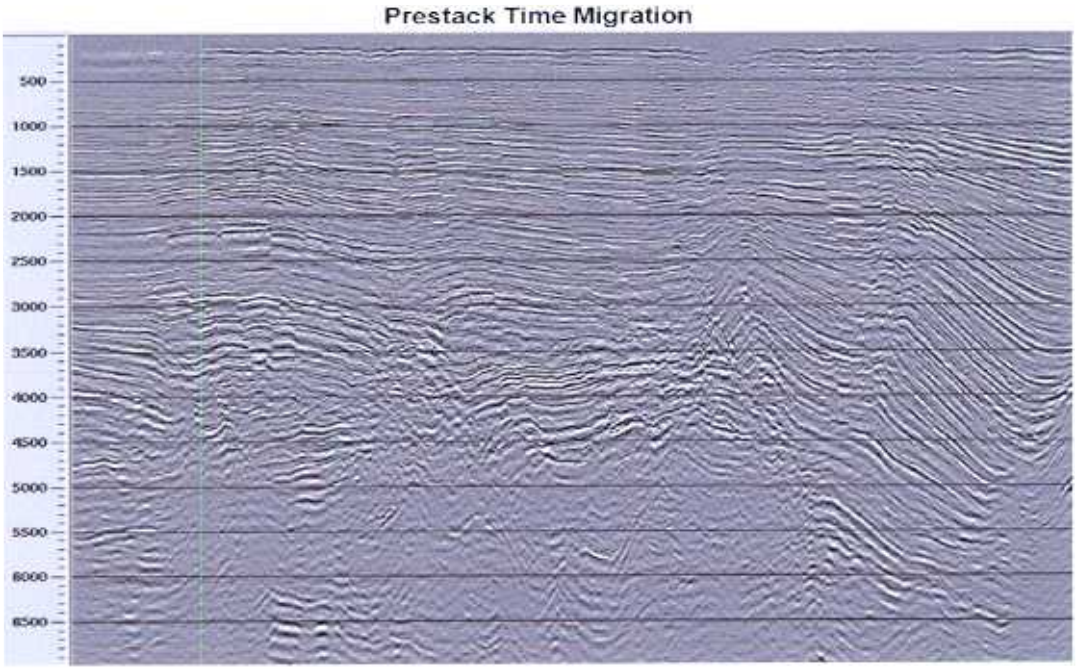

Figure 4 : Final output from 3D Kirchhoff prestack time migration In-Line 4200

References

Al-Yahya, K., 1989, Velocity analysis by iterative profile migration: Geophysics, 54, 718-729.

Audebert, F., Diet, J-P, and Zhang, X., 1996,CRP-scans from 3D pre-stack migration: a powerful combination of CRP-gathers and velocity scans: Presented at the 66th Ann.Internat. Mtg., Soc. Expl. Geophys., Expanded Abstracts 515-518.

Audebert, F., Diet, J-P, Guillaume, P., Jones, I. F., and Zhang, X., 1997,CRP-scans: 3D PSDM velocity analysis via zero-offset tomographic inversion: Presented at the 67th Ann. Internat. Mtg., Soc. Expl. Geophys., Expanded Abstracts 1805-1808.

Bleistein, N., 1987, On the imaging of reflectors in the earth: Geophysics 52, 931-942.

Farmer, P., Daube, F., Hagenes, O., Bernth, H., Sandvin, O., and Kostov, C., 1994, Representation and visualization of 3-D velocity-depth models: Presented at the 64th Ann. Internat. Mtg., Soc. Expl. Geophys., Expanded Abstracts 1253-1255.

Kosloff, D., Sherwood, J., Koren, Z., Machet, E., and Falkovitz, Y, 1996, Velocity and interface depth determination by tomography of depth migrated gathers: Geophysics, 61, 1511-1523.

Schneider, W. A., 1978, Integral formulation for migration in two and three dimensions: Geophysics, 43, 49-76.

Stewart, R. R., 1991, Exploration seismic tomography: fundamentals (Course notes series, v3): Soc. Expl. Geophys.

Stork, C., 1992, Reflection tomography in the postmigrated domain: Geophysics, 57, 680-692.

Woodward, M., Farmer, P., Nichols, D., and Charles, S., 1998, Automated 3D tomographic velocity analysis of residual moveout in prestack depth migrated common image point gathers: Presented at the 68th Ann. Internat. Mtg., Soc. Expl. Geophys., Expanded Abstracts 1218-1221.

Wyatt, K. D., Valasek, P. A., Wyatt, S. B., and Heaton, R. M., 1997, Velocity and illumination studies from horizon-based PSDM: Presented at the 67th Ann. Internat. Mtg., Soc. Expl. Geophys., Expanded Abstracts 1801-1804.